Comparative Study of Local Binary Pattern Derivatives for Low Size Feature Vector Representation in Face Recognition

Marek Loderer, Jarmila Pavlovicova, Milos Oravec

Faculty of Electrical Engineering and Information Technology, Slovak University of Technology in Bratislava, Ilkovicova 3, 812 19, Bratislava, Slovakia, e-mail: marek.loderer@stuba.sk; jarmila.pavlovicova@stuba.sk; milos.oravec@stuba.sk

Abstract: In this paper, Local Binary Patterns (LBP) and their derivatives, like Local Ternary Patterns (LTP), Local Gradient Patterns (LGP), Non-Redundant Local Binary Patterns (NRLBP) and multi-scale images processed by LBPs, are evaluated in order to find the optimal features for the automatic face recognition system. The comparison of LBP and its variations is performed based on the recognition accuracy. The genetic algorithm optimizes a criterion function, which combines four parameters, such as LBP feature type, feature image processing type, and feature dimension and distance measure. The evaluation was performed on four different face databases. The proposed methodology can be applied in various kinds of recognition, such as facial expression recognition. The main strength of this paper is the design methodology for the selection of the most discriminative features, in accordance with the desired feature vector length and face recognition accuracy.

Keywords: Face recognition; LBP (Local Binary Patterns); LTP (Local Ternary Patterns); LGP (Local Gradient Patterns); NRLBP (Non-Redundant Local Binary Patterns); Dimension reduction; Genetic algorithm; Optimal parameters selection

1 Introduction

As we know, biometrics is concerned with the automatic recognition of humans, based on their physiological or behavioral characteristics. Each face-based biometric system involves the following stages: image pre-processing, feature extraction and feature classification. In the pre-processing step the images are normalized i.e. they are cropped, resized, adjusted by a histogram equalization etc. The feature extraction process plays the crucial role in face recognition. There are many feature extraction methods based on geometry [1, 2], statistics [3, 4] or texture analysis [5, 6] which have been proposed and used in face recognition systems. The performance and accuracy of those methods may vary, however, due to varied illumination, facial expression and pose. Finally, it is decided if the subject's face matches some the faces stored in the database. There are many discriminative metrics and algorithms used in the classification process [7].

The Local Binary Pattern (LBP) as the texture descriptor was proposed in [5]. Since then many modifications of the LBPs have been published [8]. Concerning the simplicity, speed and high discriminative power of the LBPs, they have been widely used in many applications including face recognition [5, 9, 10], face detection [11, 12], human detection [6, 13], facial expression recognition [14], gender recognition [15] and face authentication [16]. There are many applications which use the LBP features for texture classification [5, 13, 14, 15], shape localization and object detection [17], or real time biometric applications in intelligent interfaces, like admission and authorization to the services in the next-generation of hybrid broadcast broadband television [18].

We propose a review study of binary pattern modifications and perform the face recognition system optimization based on different LBP features. This paper is organized as follows: Section 2 presents a brief overview of the used face databases and their properties; Section 3 is concerned with a detailed description of different LBP features and their modifications. Partition of feature images into blocks is addressed in Section 4. In Section 5, we present the different distance measures used in the study. The application of genetic algorithm for optimization of face recognition system parameters is described in Section 6. Finally, in Section 7, we discuss the results under the conditions of constrained computational complexity and suitability for devices with reduced resources.

2 Face Database

For the optimized face recognition system testing purposes, we used four standard databases. The images used were of different size, however, and thus for a valid comparison of results, it was necessary to resize them uniformly. To unify the size of input images, we applied down sampling. In our tests three different image scales are processed: 56*64 pixels, 42*48 pixels and 28*32 pixels. The summary of the databases is shown in Table 1.

The CMU PIE (Pose, Illumination and Expression) face database consists of 68 individuals [19]. For our experiments, we created training and testing sets as part of the database (according to three different poses C05, C27 and C29 shown in Fig. 1). We used 97 images per each subject (6596 samples). The original size of a sample image is 640*486 pixels. It was cropped to the size of 64*64 pixels and then resized to the final size of 56*64 pixels.

The Extended Yale Face Database B consists of 38 individuals [20]. In our research, we created training and testing sets of 64 images per subject (2432 samples). The original image size was 640*480 pixels, the cropped size 168*192 pixels and final size after being resized is 56*64 pixels.

The ORL or ATT face databases consist of 40 individuals [21]. For our experiments, we created training and testing sets using 10 images per each subject (400 samples). The original image size was 92*112 pixels and the cropped size is 56*64 pixels.

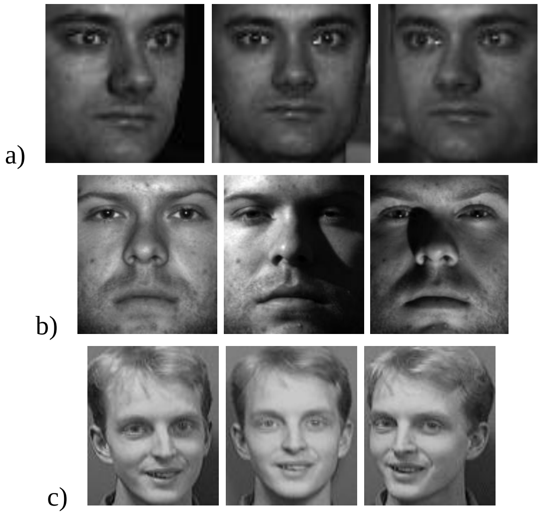

Figure 1
Examples of three different poses (C05, C27 and C29) in CMU PIE database (a); Extended Yale Face Database B (b); ATT/ORL database (c)

The FERET database contains faces with different expressions, under different illumination and a wide set of pose variations [22]. In contrast to above mentioned databases with homogeneous background where faces are already localized (Fig. 1), in the case of FERET database it was necessary to apply complex preprocessing to localize faces and remove the background (Fig. 2). In this way, our own dataset called “BIG Faces” was created. “BIG Faces” is part of the grey-scale FERET database (sets “fa” and “fb”). The images were cropped and resized using geometric normalization based on eye coordinates. As a pre-processing, the histogram equalization was applied. The irrelevant parts of images were masked using an ellipse around the face (Fig. 2). In this way, we reduced the influence of background, clothes etc. The original dimension of a sample image was 256*384 pixels, the cropped size 134*154 pixels and the resized image has 56*64 pixels.

Two different subsets (BIG4 and BIG6) were created. The BIG4 contains at least four samples per subject. There are 246 individuals and 1223 samples. The BIG6 contains at least six samples per subject. There are 73 subjects and 531 samples.

After complex preprocessing described above, localized faces with homogeneous backgrounds were used both for training and testing. The advantages of such a procedure is the increase of recognition accuracy, the reduction of the number of training images, the lowering of computational complexity, in the classification stage and improvement of the overall robustness of the system. It can be noted that preprocessing procedure does not influence the optimization process by the genetic algorithm.

Figure 2
The original image in FERET database (left) and examples of pre-processed “BIG Faces”

Table 1
Used databases

Database	Original size	Number of subjects	img/subject used	Sample numbers	Resized to
CMU PIE	640x486	68	97	6596	56x64
Ext. YALE	640x480	38	64	2432	56x64
ATT	92x112	40	10	400	56x64
FERET BIG4	256x384	246	at least 4	1223	56x64
FERET BIG6	256x384	73	at least 6	531	56x64

3 Face Feature Extraction

An optimal selection of discriminative features is an essential condition of efficient face recognition and at the same time it enables memory and time complexity reduction. In our previous analysis [23] we arrived at a conclusion that the recognition accuracy depends not only on the selected LBP feature type, but also on the size and proportions of blocks used in the LBP-feature space for a histogram construction. Because of that, we used the size and proportions of blocks in the LBP-feature space as an optimization parameter.

The maximum number of training images per subject was five. Only in the case of the BIG4 database, three training samples per each subject were used. The training samples were selected in the following two ways, using different images (inputs) and K-means clustering algorithm.

The extended YALE B, ATT/ORL and BIG Face databases contain only frontal images. The training samples were selected according to the original face images pre-processed by an adaptive histogram equalization.

In case of the CMU PIE database, better results were achieved using the LBP-feature images. We used four types of LBP and four different mappings (none, U2, RI and RIU2). These images were set as the input data for the clustering algorithm. In other words, 16 training sets were created according to the mentioned types of features. In the optimization phase, the genetic algorithm used these 16 training sets for the corresponding 16 types of the LBP features. We can assume that the selection based on the LBP-feature images used a variance of features caused by various poses (C05, C27 and C29), but not by various illumination.

3.1 LBP (Local Binary Patterns)

The original LBP operator described in [5] seems to be an efficient texture descriptor. It is robust against illumination changes and it can be computed very rapidly. The $\mathrm{LBP}_{P,R}$ operator assigns a binary value to each pixels p_i in the defined neighborhood of the central pixel p_c, where the grey-value of p_c is a threshold (Fig. 3, a-c). The result of $\mathrm{LBP}_{P,R}$ operator application is a feature image of decimal $\mathrm{LBP}_{(P,R)}$ values (1). An extended $\mathrm{LBP}_{P,R}$ operator is able to deal with the different number of samples P in the central pixel neighborhood of the radius R (Fig. 3, d,e).

$$\mathrm{LBP}_{P,R} = \sum_{i=0}^{P-1} s(p_i - p_c)2^i \tag{1}$$

$$s(x) = \begin{cases} 1, & x \geq 0 \\ 0, & x < 0 \end{cases} \tag{2}$$

a)

7	6	5
7	7	4
7	9	8

b)

1	0	0
1		0
1	1	1

c)

1	2	4
128		8
64	32	16

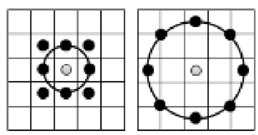

d) e)

Figure 3

$\mathrm{LBP}_{(P,R)}$ example for P=8, R=1: a) gray-level values p_i around the central pixel p_c = 7, b) binary values according to equation (1), c) corresponding powers of 2; final binary value is 10001111 and corresponding decimal $\mathrm{LBP}_{(8,2)}$ number is 241; d) $\mathrm{LBP}_{(8,1)}$, e) $\mathrm{LBP}_{(8,2)}$

Here, *s(x)* is the threshold function. One of the LPB extensions is a uniform pattern (U2). In this case the pattern corresponds with the uniform pattern if a binary string contains at most two bitwise transitions from 0 to 1 or vice versa. These patterns represent important features in such areas as spots, corners and edges. All of the other (variant) patterns are merged into one value. The other extensions of the LPB are the rotation invariant patterns (RI). In this modification, each binary number is rotated to the same normalized minimal value. The combination of both extension types represents the rotation-invariant and uniform patterns (RIU2).

3.2 LGP (Local Gradient Patterns)

The LGP was proposed to overcome the problem of local intensity variations along the edge components [6]. The LGP operator (3) is applied to the gradient magnitude image in the defined neighborhood values g_i of the central pixel with the gradient magnitude $\bar{g}$. They are computed as the absolute value differences between the intensity of the central pixel p_c and the surrounding pixel values p_i (4). Then the intensity of the central pixel p_c is substituted by the average value $\bar{g}$ (a locally adapted threshold) of all gradient values g_i (4). This value is used as the threshold value. The result value is computed from the gradient magnitude image in the same way as in case of the basic LBP operator with the same threshold function (2).

$$\mathrm{LGP_{P,R}} = \sum_{i=0}^{P-1} s(g_i - \bar{g})\, 2^i \tag{3}$$

$$g_i = |p_i - p_c| \quad \bar{g} = \frac{1}{P}\sum_{i=0}^{P-1} g_i \tag{4}$$

According to the previous definition, the LGP operator generates the following patterns. If the intensity of both the background and the foreground are changed globally (concurrently) there is no significant difference between the LGP and LBP operators (each of them generates invariant patterns). If the intensity of the background or the foreground is changed locally, the LGP generates invariant patterns in contrast to the LBP operator (generating variant patterns). This difference is caused by gradient differences (not only by intensity differences).

3.3 NRLBP (Non-Redundant Local Binary Patterns)

The NRLBP operator was proposed as a solution for the feature extraction in images with a bright object on a dark background or vice versa. The NRLBP patterns for these two types of images are different which means that the NRLBP features make distinguishing between them possible [13]. The authors proposed the pattern value as the minimum value of the LBP pattern and its complement. The greatest code becomes redundant and consequently it will occur in none of the histograms.

$$\mathrm{NRLBP}_{P,R} = \min\left(\mathrm{LBP_{P,R}}, 2^{P} - 1 - \mathrm{LBP_{P,R}}\right) \tag{5}$$

The mapping reduces the number of decimal values significantly. The disadvantage of this method is, however, that objects with different structure can get the same histogram representation.

3.4 LTP (Local Ternary Patterns)

Tan et al. in [24] extended the LBP from binary code to a three-valued code called Local Ternary Patterns. The threshold function was changed to a three-valued function as follows:

$$s(p_i, p_c, t) = \begin{cases} +1 & p_i \geq p_c + t \\ 0 & |p_i - p_c| < t \\ -1 & p_i < p_c - t \end{cases} \quad (6)$$

Here p_i are the pixel values in the neighborhood of the central pixel with the grey value p_c and t is the zone width. The LTP operator is less sensitive to noise than the LBP operator. Features generated by the LTP can be split into negative and positive parts thus reducing the computing complexity [25]. The number of histogram bins may be assigned arbitrarily. A large value leads to a huge feature vector, while a small value loses the variety of properties extracted by using the LTP operator. We set the parameter t=5 and we joined the positive and the negative parts to reduce the number of histogram bins.

3.5 Multi-Scale Images

There are many applications which use the multi-scale sampling, e.g. [26]. The multi-scale sampling has proven to be effective for face recognition and thus, we have decided to include it into our study.

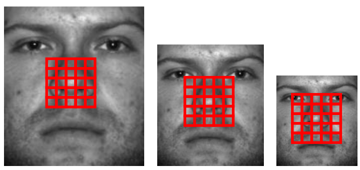

Figure 4

Multi-scale image representation. The descriptor comprehends the detail appearance in the close area of the fiducial point (the large-scale image on the left) and captures the global shape of the face (the small-scale image on the right).

We built an image pyramid of normalized images using the original image and two scaled images (Fig. 4). An advantage of multi-scale sampling is that it encodes both micro and macro structures of the subject’s face simultaneously. On the other hand, a disadvantage of this approach is the higher computational complexity [27].

3.6 Block Size Selection in LBP Feature Space

As we mentioned before, the recognition accuracy depends also on the size and proportions of blocks used in the LBP feature space for a histogram construction. We analyzed all the possible uniform image decompositions for a given input image size to find the optimal size. If the size of the original image is 56*64 pixels, then the LBP feature image after application of the LBP with P=8 and R=2, will have the size of 54*60. There are 72 different ways how to divide this image into equal blocks.

4 Parameter Optimization Based on the Genetic Algorithm

The Genetic algorithm (GA) is a stochastic algorithm that provides an efficient method of finding the global optimal solution. The GA uses a biological aspect of evolution (evolutionary computing) and is well suited for handling many computational problems [28, 29, 30, 31].

The rather important parameters of the GA algorithm are: chromosome (sequence of values which will be optimized), number of individuals in population per generation (p_g=30), number of generations (g_n=100), mutation probability (p_m=0.05), recombination probability (crossing-over) (p_r=0.5) and objective function (12) i.e. the fitness function.

The GA starts with randomly defined population (size of population – p_g). In this population each individual is represented as a chromosome. The fitness function evaluates fitness of the parameters in a chromosome. Only some chromosomes (according to the value of the fitness function and selection strategy, such as tournament strategy) are selected for reproduction. Crossing-over and mutation are used as possible ways of reproduction of new or changed chromosomes. After the new population is created, the fitness of this population will be evaluated. If the population achieves the desired fitness level or maximal number of generations (g_n), the procedure will be terminated [30].

Optimized parameters using the GA are:

- Type of 16 extracted features (with different LBP patterns mappings): LBP (none, U2, RI, RIU2); LGP (none, U2, RI, RIU2); NRLBP (none, U2, RI, RIU2) and LTP (none, U2, RI, RIU2)
- Size of blocks in feature space
- Type of distance measure (L1, L2, χ^2)

We tested three simple distance measures as the feature classification criteria.

The L1 distance is often used to compute the dissimilarity between images [7]. ***x*** and ***y*** are row vectors and N is the vector length. The same parameters are in equations (8) and (9).

$$\mathrm{L1}(x, y) = \sum_{i=0}^{N-1} |x_i - y_i| \quad (7)$$

The L2 distance (Euclidian distance) in [7] is defined as:

$$\mathrm{L2}(x, y) = \sqrt{\sum_{i=0}^{N-1} (x_i - y_i)^2} \quad (8)$$

The Chi-square (χ^2) is a statistical test for evaluation of consistency of the explored data set and a hypothetic data distribution [7].

$$\chi^2 = \sum_{i=0}^{N-1} \frac{(x_i - m_i)^2}{m_i} \quad m_i = \frac{x_i - y_i}{2} \quad (9)$$

We restricted the size of the feature vector by 1/3rd of an image size. The following objective function is optimized (minimized) by the genetic algorithm

$$f(d, x, y, acc) = 0.01 \frac{d}{Ix * Iy} + (1 - acc), \quad (10)$$

size of blocks in feature space where *d* is the number of the histogram bins, *x* and *y* are the dimensions of original image from corresponding database, I_x and I_y is the number of rows and columns of the image and *acc* is the current recognition accuracy. If $d > (I_x * I_y)/3$, this chromosome is ignored (length of feature vector is larger than 1/3rd of the image size). According to the number and size of blocks and the number of bins (concatenation of histograms) the length of the feature vector is constrained. The block diagram is shown in Fig. 5.

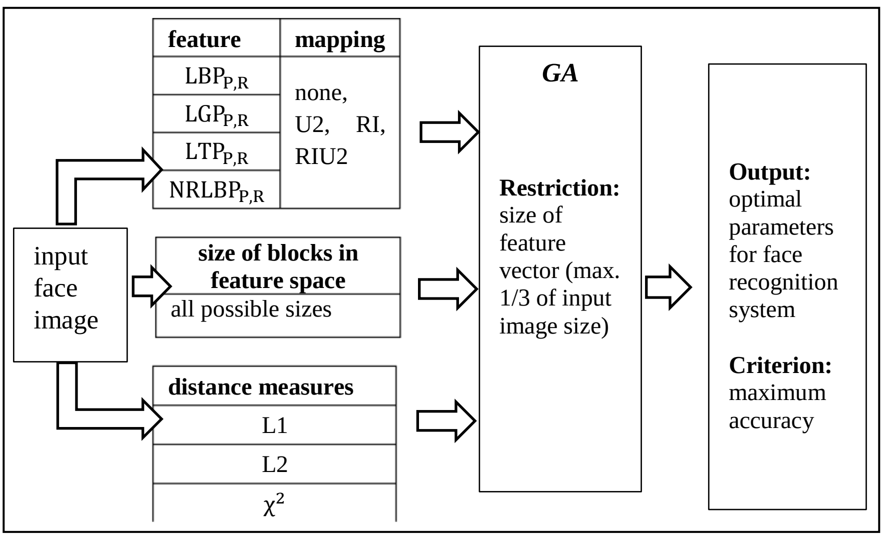

Figure 5

Block diagram of the optimization process

The optimized parameters which offer the best recognition accuracy for different face databases are shown in Tables 2-3. In case of multi-scale image approach, three different scales of images were tested. The parameters which offer the best recognition accuracy for each face database are in Table 3.

Table 2
Optimal parameters for all databases (exclusive of multi-scale images)

Database	R	Feature type	Block dimension	Feature dimension	Distance measure	Recognition accuracy
CMU PIE	3	LBP RIU2	1*25	1160	χ^2	87,274
Ext. YALE	2	LBP RIU2	2*13	1200	L1	95,079
ATT	2	LTP U2	11*38	236	L1	99,500
		LBP U2	15*52			
BIG4	2	NRLBP RIU2	6*4	1170	L1	98,316
BIG6	1	LTP RIU2	2*18	930	L1	99,096

Table 3
Optimal parameters for all databases (multi-scale images)

Database	R	Feature type	Block dimension	Feature dimension	Distance measure	Recognition accuracy
CMU PIE	3	LBP RIU2	26*22	1010	χ^2	87,675
			1*36			
			2*25			
Ext. YALE	3	LBP RIU2	26*22	720	χ^2	93,949
			1*36			
			2*50			
ATT	3	LTP U2	26*22	236	χ^2	99,500
			42*36			
			29*50			
BIG4	2	LTP RIU2	28*6	930	χ^2	98,660
			4*38			
			10*4			
BIG6	3	LTP RIU2	2*22	1130	L1	99,498
			7*6			
			2*50			

In either case, we applied three values of a pixel neighborhood radius (R). The feature type and mapping (Feature type), the number of columns and rows of one texture block (Block dimension) and the distance measure are parameters optimized with respect to the achieved recognition accuracy and length of the feature vector. The feature vector dimension (Feature dimension) is restricted and must not exceed one third of the image size. In most cases the maximum length of a feature vector was reached as an optimum. 6-fold cross validation was performed and an average recognition accuracy (Recognition accuracy) is shown in the following tables.

5 Experimental Results

The best results were achieved for the image size of 64*56 pixels. Only in case of the ATT database, the LTP U2 features were obtained from the image size of 48*42 pixels (the first row in Table 2) and the LBP U2 features were extracted from the image size of 64*56 pixels (the second row in Table 2).

The LBP, as well as the LTP features achieved the best recognition accuracy. The LBP can be commonly used in numerous applications. On the other hand, even if the LTP is able to reduce the influence of noise in images, its disadvantage is the significant data correlation between its positive and negative parts. Although R=2 is used in most publications, in our optimization process R=3 can be considered a more suitable alternative, especially in case of a multi-scale image approach. Both the rotation invariant and uniform patterns (RIU2) and uniform patterns (U2) occur mostly in optimal parameter sets. The RIU2 offers such advantages as significant dimension reduction, rotation invariance and identification of significant face features. The U2 patterns, however, are more suitable for face recognition.

From the three tested simple and fast distance measures, the χ^2 distance occurred most frequently in optimization processes. Still, L1 distance provides favorable classification results.

Obviously, the multi-scale images increase the recognition accuracy (PIE=+0.40%, BIG6=+0.40%, BIG4=+0.34%, ATT without change and Extended YALE=–1.13%, but there was significant dimension reduction).

In case the face database is rather small, a short vector of features (ATT length of vector is 236) is sufficient. Larger databases, however, need at least 930 features to achieve the desired accuracy.

The database size, number of subjects per database and different poses have a considerable influence on the size and shape of blocks. The shape and size of blocks are varying in case of image scaling. There are thin horizontal stripes (PIE – 1*25, ATT – 11*38 pixels) or small rectangular areas (Extended YALE – 2*13, BIG6 – 2*18 pixels) or small, almost squared, areas (BIG4 – 6*4 pixels). The scaled version contains three different image sizes. There are also thin horizontal stripes (PIE – 1*36, Extended YALE – 1*36, 2*50, BIG4 – 4*38, BIG6 – 2*22, 2*50 pixels), then the rectangular areas (PIE – 2*25, BIG4 – 28*6, 10*4 pixels) and finally the almost square areas (BIG6 – 7*6 pixels). In this case also the whole images were used as input image blocks (PIE, Extended YALE, ATT – 26*22 and ATT – 42*36 pixels).

In Tab. 4, we compared the results obtained by us with the state-of-the-art contributions. The proposed methods with the best results, which were evaluated on the mentioned databases, are listed in the Table. There are many differences e.g. number of training and testing samples, size of input images and length of the feature vector.

Table 4
Comparison of achieved results with the state-of-the-art contributions

Database	References	Accuracy	Feature vector length	Proposed method (Feature vector length)
FERET (fb)	[32], 2012	99.60	1180	98,660 (930)
	[33], 2014	99.90	--	
	[34], 2015	99.90	1196	
	[35], 2015	98.58	1000	
	[36], 2016	99.60	2000	
FERET (fc)	[32], 2012	99.50	1180	
	[33], 2014	100.00	--	
	[34], 2015	100.00	1196	
	[35], 2015	100.00	1000	
	[36], 2016	100.00	2000	
FERET (-)	[37], 2014	99.00	--	
FERET	[38], 2007	93.16	--	99,498 (1130)
ATT	[38], 2007	98.50	--	99,500 (236)
	[39], 2013	≈98.70	--	
Ext. YALE	[24], 2010	99.28	≈25000	95,079 (1200)
	[40], 2014	≈96.00	≈100000	
	[41], 2015	99.34	767	
	[42], 2015	97.39	≈25000	
CMU PIE	[43], 2013	99.85	≈65000	87,675 (1010)
	[40], 2014	≈91.40	≈8000	
	[44], 2016	97.44	≈20000	

We find the proposed method which reduces data dimension significantly to be our main contribution If the authors of a method did not mention a specific number of features, we use “-” label. If there were many clues in a paper, we estimate the number of features and their number (or accuracy) has the sign “≈”.

In case of the FERET database, we achieved different results between -1.34 and +0.08%. The difference is acceptable if we take into account a slightly larger number of features.

In case of the ATT database, we achieved an improvement of +0.8%.

For larger databases, like the Extended YALE B, the obtained results show differences between -4.26 and -0.921%. As mentioned above, the feature vector dimension is considered an important parameter from the point of view of computational complexity. Yet, from Table 4 clearly follows that our result was achieved with significantly smaller feature vectors.

For the fourth database, (CMU PIE) the differences in recognition accuracy are in the interval -12.18 and -3.73%. This was caused by a significant data dimension reduction and by the influence of database size and different poses.

As shown in Table 4, we can claim that the methodology proposed by us can be used in devices with reduced sources (weak CPU or small memory). The results achieved by us are comparable with recently proposed rather sophisticated algorithms with much higher computational complexity. There is one more advantage of our approach represented by a possibility of adding a new subject to, or removing old user data from a database of features in an easy way.

Conclusions

This paper presents a new method of feature extraction for a face recognition system, optimized by the genetic algorithm. The system is optimized to achieve the desired recognition accuracy for a limited length of the feature vector. In most cases, the best recognition accuracy was achieved by the LBP patterns with the RIU2 mappings. Still, the LTP with the same mapping should be also considered as suitable for face recognition purposes. L1 and χ^2 distances are suitable and they achieved the highest recognition accuracy. The number, shape and size of blocks were also optimized using the genetic algorithm.

Taking into account the previous results (Table 2), we came to the following conclusions. The optimal size of an input image is 64*56 pixels when the parameters P=8 and R=2 are applied. With smaller images the recognition accuracy decreases. The L1 distance was selected as the optimal distance. The LGP features as such were not discriminative enough for the recognition purposes.

The rows in Table 3 show that the image pyramid improved the recognition accuracy, if the parameters P=8 and R=3 were used. χ^2 distance measure was selected as the optimal measure. It achieved the best recognition accuracy and it occurred most frequently in our optimization results.

Acknowledgement

The research described in the paper was done within the grant No. 1/0867/17 of the Slovak Grant Agency VEGA.

References

[1] Hanmandlu, M., Gupta, D., and Vasikarla, S.: Face recognition using Elastic bunch graph matching. Applied Imagery Pattern Recognition Workshop, 2013, pp. 1-7

[2] Badakhshannoory, H., Safayani, M. and Manzuri-Shalmani, M. T.: Using geometry modeling to find pose invariant features in face recognition, ICIAS, 2007, pp. 577-581

[3] Xu, Z., Wang, L. and Yang, L.: A Simulated Annealing and 2DPCA Based Method for Face Recognition, IEEE Conf. on Signal-Image Technologies and Internet-based System, 2007, pp. 777-782

[4] Martinez, A. M. and Kak, A. C.: PCA versus LDA, IEEE Trans. Pattern Analysis and Machine Intelligence, Vol. 23, 2001, pp. 228-233

[5] Ojala T., Pietikainen, M. and Maenpaa, T.: Multiresolution Gray Scale and Rotation Invariant Texture Classification with Local Binary Pattern, IEEE Transaction on PAMI, Vol. 24, No. 7, 2002, pp. 971-987

[6] Jun, B., Choi, I. and Kim, D.: Hybridization for Accurate Face and Human Detection, Pattern Analysis and Machine Intelligence, Vol. 35, No. 6, 2013, pp. 1423-1436.

[7] Zhang, D. and Lu, G.: Evaluation of similarity measurement for image retrieval, Neural Networks and Signal Processing, Vol. 2, 2003, pp. 928-931

[8] Huang, D., Shan, C., Ardabilian, M., Wang, Y. and Chen, L.: Local Binary Patterns and Its Application to Facial Image Analysis: A Survey, IEEE Transactions on Systems, Man and Cybernetics, Vol. 41, No. 6, 2011, pp. 765-781

[9] Xuefeng, Ch., Fei. L. and Huang, Ch.: Face Recognition by Zero-Ratio Based LGBP Features, World Congress on Intelligent Control and Automation, 2014, pp. 5605-5608

[10] Binbin, W., Xinjie, H., Lisheng, Ch., Jingmin, C. and Yunqi, L.: Face Recognition Based on the Feature Fusion of 2DLDA and LBP, International Conference on Information, Intelligence, Systems and Applications, 2013, pp. 1-6

[11] Bilaniuk, O., Fazl-Ersi, E., Laganière, R., Xu, Ch., Laroche, D. and Moulder, C.: Fast LBP Face Detection on low-power SIMD architectures, IEEE Conference on Computer Vision and Pattern Recognition Workshops, 2014, pp. 630-636

[12] Kadir, K., Kamaruddin, M. K., Nasir, H., Safie, S. I and Bakti, Z. A. K.: A Comparative Study between LBP and Haar-like features for Face Detection Using OpenCV, International Conference on Engineering Technology and Technopreneuship, 2014, pp. 335-339

[13] Satpathy, A., Jiang, X. and Eng, H.: Human Detection Using Discriminative and Robust Local Binary Pattern, ICASSP, 2013, pp. 2376-2380

[14] Abdulrahman, M., Gwadabe, T. R., Abdu F. J. and Eleyan, A.: Gabor Wavelet Transform Based Facial Expression Recognition Using PCA and LBP, Signal Processing and Communications Applications Conference, 2014, pp. 2265-2268

[15] Huynh, T., Min, R. and Dugelay, J. L.: An Efficient LBP-based Descriptor for Facial Depth Images applied to Gender Recognition using RGB-D Face Data, Workshop on Computer Vision with Local Binary Pattern Variants (ACCV), 2012, pp. 1-12

[16] Ouamane, A., Messaoud, B., Guessoum, A., Hadid, A. and Cheriet, M.: Multi Scale Multi Descriptor Local Binary Features and Exponential Discriminant Analysis for Robust Face Authentication, IEEE International Conference on Image Processing, 2014, pp. 313-317

[17] Ngoc, T. N.: An Efficient LBP-Based Descriptor for Real-Time Object Detection, IEEE Symposium on Computational Intelligence for Security and Defense Applications, 2014, pp. 1-5

[18] Ban, J., Pavlovičová, J., Féder, M., Omelina, L. and Oravec, M.: Face Recognition Methods for Multimodal Interface. 5th joint IFIP Wireless and Mobile Networking Conference, 2012, pp. 110-113

[19] Sim, T., Baker, S. and Bsat, M.: The CMU Pose, Illumination, and Expression (PIE) database, Proceedings of the IEEE International Conference on Automatic Face and Gesture Recognition, 2002, pp. 46-51

[20] Belhumeur, P. N., Hespanha, J. P. and Kriegman, D. J.: Eigenfaces vs. Fisherfaces: Recognition Using Class Specific Linear Projection, IEEE Transactions on Pattern Analysis and Machine Intelligence, Vol. 19, No. 7, 1997, pp. 711-720

[21] Samaria, F. S. and Harter, A. C.: Parameterisation of a stochastic model for human face identification, 2nd IEEE Workshop on Applications of Computer Vision, 2000, pp. 138-142

[22] Phillips, P. J., Moon, H. Rauss, P. and Rizvi, S. A.: The FERET evaluation methodology for face recognition algorithms, IEEE Transactions on PAMI, Vol. 22, No. 10., 2000

[23] Loderer, M. and Pavlovičová, J.: Optimization of LBP Parameters, 56th International Symposium ELMAR, 2014, pp. 1-4

[24] Tan, X. and Triggs, B.: Enhanced local texture feature sets for face recognition under difficult lighting conditions. IEEE Transactions on Image Processing, Vol. 19, No. 6. 2010, pp. 1635-1650

[25] Jia, X., Yang, X., Zang, Y., Zhang, N., Dai, R., Tian, J., Zhao, J.: Multi-scale Block Local Ternary Patterns for Fingerprints Vitality Detection, International Conference on Biometrics, 2013, pp. 1-6

[26] Chan, Ch., Kittler, J. and Messer, K.: Multi-scale local binary pattern histograms for face recognition, Advances in biometrics, 2007, pp. 809-818

[27] Chen, D., Cao, X., Wen, F. and Sun, J.: Blessing of Dimensionality: High-dimensional Feature and Its Efficient Compression for Face Verification, IEEE Conference on Computer Vision and Pattern Recognition, 2013, pp. 3025-3032

[28] Pereira, E., Gomes, H., Moura, E., Carvalho, J. and Zhang, T.: Investigation of Local and Global Features for Face Detection, IEEE Symposium on Computational Intelligence for Multimedia, Signal and Vision Processing, 2011, pp. 114-121, 2011

[29] Omelina, Ľ. and Oravec, M.: Universal biometric evaluation system: Framework for testing evaluation and comparison of biometric methods, IEEE Int. Conference on Systems, Signals and Image Processing. 2011

[30] Devi, G. S. and Rabbani, M. M. A.: Optimizing Modular Image PCA using Genetic Algorithm for Expression – Invariant face recognition, International Conference on Networks & Soft Computing, 2014, pp. 319-323

[31] Sekaj, I.: Control algorithm design based on evolutionary algorithms. In Introduction to Modern Robotics, iConcepts Press Ltd., 2011, pp. 251-266

[32] Nguyen, T. P., Vu, N. and Caplier, A.: Face Recognition using Multi-modal Binary Patterns. International Conference on Pattern Recognition, 2012, pp. 2343-2346

[33] Jain, V., Crowley, J. L. and Lux, A.: Local Binary Patterns Calculated Over Gaussian Derivative Images. International Conference on Pattern Recognition, 2014, pp. 3987-3992

[34] Lu, J., Liong, V. E. and Zhou, J.: Simultaneous Local Binary Feature Learning and Encoding for Face Recognition. International Conference on Computer Vision, 2015, pp. 3721-3729

[35] Low, Ch.: Learning Compact Discriminant Local Face Descriptor with VLAD. Asia-Pacific Signal and Information Processing Association Annual Summit and Conference, 2015, pp. 825-833

[36] Xi, M., Chen, L., Polajnar, D. and Tong, W.: Local Binary Pattern Network: A Deep Learning Approach For Face Recognition. International Conference on Image Processing, 2016, pp. 3224-3228

[37] Nikan, S. and Ahmadi, M.: Effectiveness of Various Classification techniques on Human Face Recognition. International Conference on High Performance Computing & Simulation, 2014, pp. 651-655

[38] Liao, S. and Chung, A.: Face Recognition by Using Elongated Local Binary Patterns with Average Maximum Distance Gradient Magnitude. Conference on Computer Vision, 2007, pp. 672-679

[39] Wang, B., Li, W. and Liao, Q.: Face recognition based on nonsubsampled contourlet transform and block-based kernel Fisher linear discriminant. IEEE International Conference on Acoustics, Speech and Signal Processing (ICASSP) 2012, pp. 1533-1536

[40] Fan, K. and Hung, T.: A Novel Local Pattern Descriptor - Local Vector Pattern in High-Order Derivative Space for Face Recognition. IEEE Transactions on Image Processing, Vol. 23, No. 7, 2014, pp. 2877-2891

[41] Juneja, K., Verma, A., and Goel, S.: An Improvement on Face Recognition Rate using Local Tetra Patterns with Support Vector Machine under varying Illumination Conditions. International Conference on Computing, Communication & Automation, 2015, pp. 1079-1084

[42] Yang, Z., Jiang, Y., Wu, Y., Lu, Z., Li, W. and Liao, Q.: Weber Binary Pattern and Weber Ternary Pattern for Illumination-Robust Face Recognition. Asia-Pacific Signal and Information Processing Association Annual Summit and Conference, 2015, pp. 1050-1053

[43] Ren, J., Jiang, X. and Yuan, J.: Relaxed local ternary pattern for face recognition. International Conference on Image Processing, 2013, pp. 3680-3684

[44] Chakraborty, S., Singh, S. and Chakraborty, P.: Local Gradient Hexa Pattern: A Descriptor for Face Recognition and Retrieval. Transactions on Circuits and Systems for Video Technology, 2016, pp. 1-6